

XMM–Newton EPIC and OM observation of Nova Centauri 1986 (V842 Cen)

G. J. M. Luna,^{1,2★†} M. P. Diaz,³ N. S. Brickhouse⁴ and M. Moraes³

¹*Instituto de Astronomía y Física del Espacio (IAFE/Conicet), CC67, Suc. 28 C1428ZAA Caba, Argentina*

²*Instituto de Ciencias Astronómicas, de la Tierra y del Espacio, Av. España Sur 1512, J5402DSP San Juan, Argentina*

³*IAG, Universidade de São Paulo, Rua do Matão, 1226, São Paulo, SP 05508-900, Brazil*

⁴*Harvard–Smithsonian Center for Astrophysics, 60 Garden Street, Cambridge, MA 02138, USA*

Accepted 2012 March 19. Received 2012 March 5; in original form 2012 January 19

ABSTRACT

We report the results from the temporal and spectral analysis of an *XMM–Newton* observation of Nova Centauri 1986 (V842 Cen). We detect a period at 3.51 ± 0.4 h in the EPIC data and at 4.0 ± 0.8 h in the Optical Monitor (OM) data. The X-ray spectrum is consistent with the emission from an absorbed thin thermal plasma with a temperature distribution given by an isobaric cooling flow. The maximum temperature of the cooling flow model is $kT_{\max} = 43_{-12}^{+23}$ keV. Such a high temperature can be reached in a shocked region and, given the periodicity detected, most likely arises in a magnetically channelled accretion flow characteristic of intermediate polars. The pulsed fraction of the 3.51-h modulation decreases with energy as observed in the X-ray light curves of magnetic cataclysmic variables, possibly due either to occultation of the accretion column by the white dwarf body or phase-dependent to absorption. We do not find the 57-s white dwarf spin period, with a pulse amplitude of 4 mmag, reported by Woudt et al. in either the OM data, which are sensitive to pulse amplitudes $\gtrsim 0.03$ mag, or the EPIC data, sensitive to pulse fractions $p \gtrsim 14 \pm 2$ per cent.

Key words: novae, cataclysmic variables – X-rays: general.

1 INTRODUCTION

Cataclysmic variables (CVs) are binary systems consisting of a white dwarf primary and a secondary that transfers mass to it through an accretion disc around the white dwarf. Their brightness can change by large factors (several millions) during nova outbursts, which are due to thermonuclear runaways of the hydrogen-rich material that has accreted on to the white dwarf.

The power spectra of CVs display several different periodicities which are attributed to the orbital period, white dwarf spin period (in the case of magnetic CVs) and superhumps (which are photometric modulations near, but not at, the orbital period) among others. Among magnetic CVs, intermediate polars (IPs) are moderately strong X-ray sources ($L_X \sim 10^{31}–10^{33}$ erg s^{−1}), in which accreting material is magnetically channelled and shock heated in the accretion column, producing high-energy radiation as it cools before reaching the white dwarf surface. Strong X-ray modulation is observed at the spin period, likely due to self-occultation of the accretion column by the white dwarf’s body and/or phase-dependent

absorption by pre-shock material (e.g. Allan, Hellier & Beardmore 1998).

Nova Centauri 1986 (V842 Cen) underwent its latest nova outburst in 1986 February and took 48 d to decline its brightness by 3 mag, which suggests that it was a moderately fast nova (Sekiguchi et al. 1989). Downes & Duerbeck (2000) imaged the nova ejecta in 1998 using H β and [O III] λ 5007 narrow-band filters. The ejecta show a fairly spherical shape in both filters (5.6×6.0 arcsec²). Given this information, therefore, nothing is particularly peculiar about this nova. However, optical photometry observations in 2008 overturned this picture when a fast pulsation of 57 s was discovered by Woudt et al. (2009) and attributed to the spin period of the white dwarf, which would make V842 Cen a member of the IP class. This finding has strong implications: its white dwarf would be the fastest rotator currently known in a nova remnant and its symmetric shell morphology would now present a puzzle, since a magnetic field anchored to a rapidly rotating white dwarf would be likely to produce asymmetric ejecta shapes during a nova event (Fiedler & Jones 1980; Livio 1995).

In this Letter we show the results of an *XMM–Newton* X-ray and optical observation aimed to search for the 57-s spin period discovered by Woudt et al. (2009) and thus confirm the IP nature of V842 Cen. In Section 2 we present the details of the observation and

★E-mail: gjmluna@iafe.uba.ar

data processing, while in Section 3 we show the results obtained from the timing and spectral analysis. Discussion and conclusions are presented in Section 4.

2 OBSERVATIONS AND ANALYSIS

We observed V842 Cen with the *XMM-Newton* Observatory on 2011 February 24 for 56.9 ks using the EPIC instrument, operated in full window mode with the medium thickness filter and the Optical Monitor (OM) in fast mode. After removing events at periods with high flaring particle background using a 3σ clipping method, the resulting exposure time reduced to 49.8 ks.

The source spectra and light curves were accumulated from circular regions of 32 and 20 arcsec, respectively, centred on V842 Cen ($\alpha = 14^{\text{h}}35^{\text{m}}52^{\text{s}}.55$, $\delta = -57^{\circ}37'35''.3$). The background spectra and light curves were extracted from a source-free region on the same chip taken within a circle of 40-arcsec radius. The total number of counts in the source region in the pn, MOS1 and MOS2 cameras was 5354 which includes 735 counts from background. We used the `RMFGEN` and `ARFGEN` to build the redistribution matrices and ancillary responses, respectively. The resulting X-ray spectra were grouped with a minimum of 15 counts per energy bin. For timing analysis, we converted photon arrival times to the Solar system barycentre using the `SAS` task `barycen`. The exposure times in the OM filters were 16594, 16599 and 16596 s for the V, U and B, respectively. The OM light curves were reprocessed using the script `omfchain` with time bin size of 0.5 s.

3 RESULTS

3.1 Timing

For the X-ray data, we used the event arrival times and Rayleigh statistics (Z_1^2 ; Buccheri et al. 1983; Stute, Luna & Sokolowski 2011) to search for periods in the frequency range from $f_{\text{min}} = 1/T_{\text{span}}$ to $f_{\text{max}} = 1/2t_{\text{frame}}$, with $\Delta f = 1/AT_{\text{span}}$, where T_{span} is the total on-source time of 49.8 ks, t_{frame} is the EPIC camera readout time (73 ms) and A is the oversampling factor, which we set equal to 1000. We detect a period at 3.64 ± 0.46 h which is within the errors of the ~ 3.94 h orbital period (Fig. 1) estimated by Woudt et al.

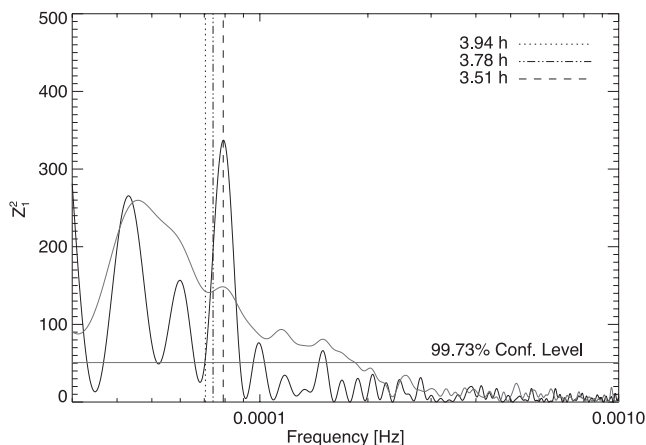


Figure 1. Power spectrum $Z_1^2(f)$ from the source+background (black) and background (red) photon arrival times from the pn+MOS1,2 cameras. The 99.73 per cent (3σ) confidence level is marked by the horizontal line (red). Vertical dotted, dot-dashed and dashed lines show the 3.94-, 3.78- and 3.51-h periods, respectively. A colour version of this figure is available online.

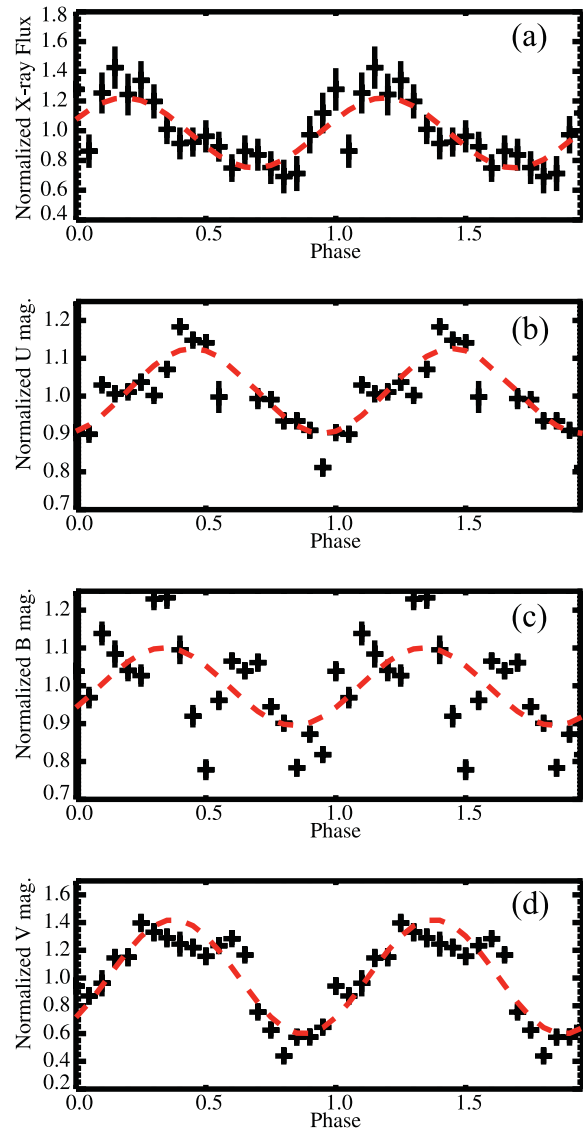


Figure 2. (a) EPIC/pn light curve in the 0.3–10 keV energy range folded at the 3.5-h period. Normalized U (b), B (c) and V (d) magnitude light curves folded at the 3.51-h period. A sine wave fit of the form $A + B \times \sin[2\pi(\phi_{3.51} - \phi_0)]$, where $\phi_{3.51}$ is the phase at the 3.51-h period, is overlotted (dashed line). Each point corresponds to an average over a 0.05 phase bin. A colour version of this figure is available online.

(2009). We are not able to detect the ~ 57 s white dwarf spin period in the X-ray data.

Since the particle background is not expected to be modulated, it should be safe to use all the exposure time (56.9 ks) to improve the accuracy of the period detection. In this case, the modulation is found to have a period of 3.51 ± 0.40 h. These data are sensitive to pulse fractions¹ $p = 14 \pm 2$ per cent (using equation 3 from Stute et al. 2011). In Fig. 2(a) we show the pn light curve in the 0.3–10.0 keV energy range phased at the 3.51-h period. We choose the ephemeris $T_0 = \text{HJD } 245\,4514.548\,82$, which is the date of the first photometric observation reported by Woudt et al. (2009).

¹ We define the pulsed fraction p as $\text{max}/\text{min} = (A + B)/(A - B)$, where A and B are determined from a sine wave fit of the form $A + B \times \sin[2\pi(\phi_{3.51} - \phi_0)]$, where $\phi_{3.51}$ is the phase at the 3.51-h period.

Due to the period uncertainty, our phase scale is arbitrary and cannot be compared with previous works.

The U , B and V light curves were scanned for periodicities ranging from 1 s to 5 h. Fourier transform and phase dispersion minimization algorithms were used in order to detect sinusoidal as well as complex pulse profiles. No pulsed signal with semi-amplitude above 0.03 mag could be found in the 1–1000 s period range in U , B and V bands. In particular, no significant peak appears at the 57-s period attributed to the white dwarf spin; however, we note that the pulse amplitude of 4 mmag measured by Woudt et al. (2009) is below our detection limits. The most significant structures in the mid-frequency range are located in the range between 27 and 32 min. Their coherence could not be verified and they may just represent the flickering time-scale in this system. After rebinning to 100-s integrations, a 4.0 ± 0.8 h period is clearly seen in our light curves, with one complete cycle covered in U , B and V on different occasions. Simulations show that a sinusoidal semi-amplitude of 0.13, 0.10 and 0.14 mag can be measured in U , B and V bands, respectively, for a 4.0-h trial period. Phase-folded light curves in the OM filters shows significant departures from a sinusoidal shape that may be due to flickering activity during the cycle sampled by our observations (Fig. 2). The light curves in each filter show significant change between cycles at particular phases. These changes appear as regions of larger scatter in the phase-binned curves.

The individual OM light curves sample less than two photometric cycles. Therefore, the broad peak at low frequencies (with maximum between 3 and 4 h) includes the 2.889-h period claimed by Woudt et al. (2009) at a high power level, producing reasonable phase-folded light curves. However, longer optical data sets are needed to study the orbital/superhump modulations and the low-frequency domain.

3.2 Spectrum

The X-ray spectrum of V842 Cen is relatively hard with photon energies up to $\gtrsim 10$ keV (Fig. 3). Visual inspection shows an emission feature at energies ~ 6.7 – 7.0 keV which corresponds to Fe_{XXV} and Fe_{XXVI} . A simple thermal model ($\chi^2 = 297$,

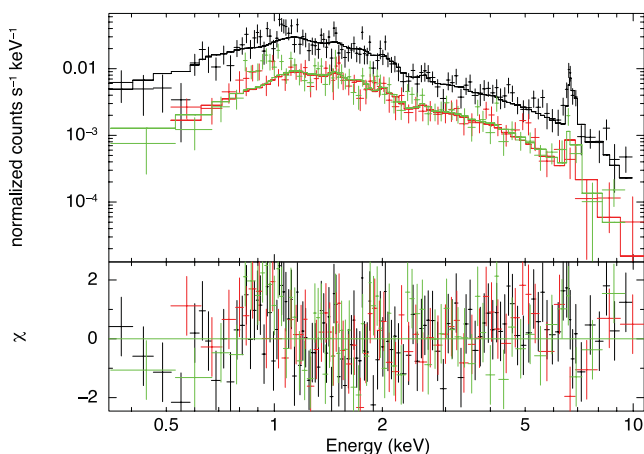


Figure 3. XMM EPIC background-subtracted spectra (pn in black, MOS 1 in red and MOS 2 in green). The best-fitting absorbed cooling flow model is overplotted in the top panel. Bottom panel shows fit residuals. A colour version of this figure is available online.

271 d.o.f.) of an absorbed plasma ($\text{wabs} \times \text{APEC}$ in XSPEC^2) yields a temperature $kT = 8.1_{-1.0}^{+1.6}$ keV, an absorption column density $n_{\text{H}} = 0.25_{-0.03}^{+0.03} \times 10^{22} \text{ cm}^{-2}$ and abundance $A = 2.0_{-0.5}^{+0.7}$ in solar units.

Given the detection of a modulation in the X-ray light curves, we also fit the spectrum with models successfully applied to cooling accretion shock columns, in which the temperature distribution depends on the cooling mechanisms (e.g. Allan et al. 1998). In the simplest scenario, the X-ray spectrum can be modelled with an isobaric cooling flow (e.g. Mukai et al. 2003; Pandel et al. 2005). We use the mkcflow model (with the switch parameter equal 2, meaning that the model spectrum used the APEC emissivities) modified by a simple absorber (wabs). The model fit ($\chi^2 = 260$, 267 d.o.f.) results in a maximum plasma temperature $kT_{\text{max}} = 43_{-12}^{+23}$ keV, a minimum temperature $kT_{\text{min}} \lesssim 0.6$ keV, absorption column $n_{\text{H}} = 0.30_{-0.04}^{+0.04} \times 10^{22} \text{ cm}^{-2}$, abundance $A \geq 2$ in solar units and mass accretion rate $\dot{M}(10^{-12}) = 7_{-2}^{+2} \text{ M}_{\odot} \text{ yr}^{-1}$ ($d/1.3 \text{ kpc}$)² (using the distance from Gill & O’Brien 1998).

At the accretion shock front, the shock temperature is proportional to the square of the free-fall velocity, which in turn is set by the mass of the white dwarf. Thus the white dwarf mass can be derived from the value of kT_{max} obtained from fitting the spectrum with a cooling flow model (e.g. Yuasa et al. 2010). The value of kT_{max} obtained from our fit implies $M_{\text{WD}} = 0.88 \text{ M}_{\odot}$, where M_{WD} is the mass of the white dwarf.

4 DISCUSSION AND CONCLUSIONS

The nature of V842 Cen remains unclear. Optical data obtained in 2008 show modulations at 56.825 s and 3.780 ± 0.004 h (Woudt et al. 2009). These authors attributed the shorter period to the white dwarf spin. The presence of sidebands at 56.598 and 57.054 s suggested that the orbital period should be at 3.94 h. In this picture, they then attributed the 3.780-h period to a ‘negative superhump’, a hump-shaped feature in the light curve with period a few per cent less than the orbital period of the binary. Superhumps are believed to be associated with a tilted accretion disc. This analysis strongly suggests that V842 Cen should be classified as an IP. It is somewhat puzzling why earlier fast optical photometry of V842 Cen did not show periodicity (Woudt & Warner 2003); presumably, flaring activity observed in that data masked any periodic signatures. Our data cannot confirm the short period at X-ray or optical wavelengths. While the lack of a ~ 57 s period in the X-ray data does not necessarily rule out a rapidly rotating white dwarf, one generally expects the X-ray data from IPs to be modulated at the spin period, since the localized accretion shock near the surface of the white dwarf produces a high-temperature thermal spectrum. Unfortunately, our optical data are not sensitive enough to detect a pulse amplitude of 4 mmag as previously measured.

On the other hand, we detect significant periods at 3.51 ± 0.40 h in X-rays and 4.0 ± 0.8 h in optical. The pulsed fraction p of the X-ray light curves folded at this period decreases with energy, ranging from 47 ± 13 per cent in the soft X-ray band (0.3–1.0 keV) to 45 ± 12 per cent in the medium X-ray band (1.0–2.0 keV) and to 30 ± 11 per cent in the hard X-ray band (2.0–10.0 keV). A similar trend is observed in the X-ray spin-phased light curves of IPs (e.g. EX Hya; Allan et al. 1998) and can be caused by the energy dependence of the absorption cross-section, occultation of the lower (cooler)

² <http://heasarc.gsfc.nasa.gov/docs/xanadu/xspec/>; APEC models from Smith et al. (2011); wabs model from Morrison & McCammon (1983).

portion of the accretion column by the white dwarf's body or both. The modulation detected in our data is somehow different from the orbital period claimed by Woudt et al. (2009) at the 3σ level. Furthermore, the smooth shape of the phase-folded light curves indicates that an orbital origin of the modulation is unlikely. A low orbital inclination as suggested by Woudt & Warner (2003) also supports this conclusion. Eclipses of the accretion column are observed as sharp decreases in the light curves of IPs with high orbital inclination (Hoogerwerf, Brickhouse & Mauche 2005), lasting for tenths or less of the orbital period. No conspicuous eclipse feature could be found using a 50-s binning in any of the light curves.

On the other hand, the period we have detected is consistent with the value reported by Woudt et al. (2009) as a negative superhump; however, it is not clear how the tilted accretion disc would contribute to such high-energy X-ray emission. To our knowledge, negative superhumps have not been detected in a CV at X-ray wavelengths. Furthermore, the energy dependence of the pulsed fraction of an X-ray superhump would require explanation.

The X-ray spectrum is fully consistent with thermal emission originating in the post-shock region of a magnetic accretion column (e.g. Mukai et al. 2003). The model fit to the X-ray spectrum suggests that the white dwarf in V842 Cen has a mass $M_{\text{WD}} = 0.88 M_{\odot}$, which is not unusual for an IP. In fact, Brunschweiler et al. (2009) found that among the IPs detected with *Swift*/BAT, five out of 17 have white dwarfs more massive than $0.88 M_{\odot}$. Given the good agreement with the accretion shock model and a reasonable mass determination, it is difficult to reconcile the lack of detection of the fast period associated with the white dwarf spin. Either the fast period is undetectable due to a low inclination or the period we detect is instead the white dwarf spin period. The latter possibility would be, if confirmed, very rare since the detected period is longer than any known spin periods from IPs.³

The shape of the nova remnant in V842 Cen also remains puzzling. The remnant geometry depends on the matter distribution and the ejecta illumination by the central source. If no accretion disc is present in V842 Cen (e.g. it is a polar CV instead of an IP), then the ejecta might be more homogeneously illuminated; however, at the moment we do not think that this is a possibility as no evidence has been reported elsewhere on the detection of optical polarization or strong soft X-ray emission that would support the polar nature. One expects the presence of a large accretion disc to affect the photoionization in different regions of the nebula. The accretion disc may absorb the ionizing photons in the equatorial regions causing an aspherical illumination. In HR Del, for example, the observed aspherical illumination is attributed to high mass transfer and a large disc (Moraes & Diaz 2009).

Furthermore, a high white dwarf rotational velocity can generate asymmetries in the eruption conditions because of the effective gravity variation from equatorial to polar regions (Scott 2000). If we consider a $0.88 M_{\odot}$ white dwarf with a rotational period of 57 s, we should obtain ejecta with axial ratio of ~ 1.35 (using expressions

8–11 by Scott 2000). If the rotational period is 3.51 h, the envelope would be symmetric. A period $P \lesssim 125$ s is required to detect an asymmetric envelope. If the white dwarf is more massive than what we have derived, the asymmetry would be smaller, but detectable (as a prolate remnant).

In summary, the X-ray spectrum and the energy dependence of its pulse fraction support the classification of V842 Cen as an IP, but the symmetric shape of the ejecta and the long period of the light curves are not easily explained in this picture. While the X-ray data do not definitively rule out a very fast 57 s spin period, a longer period would be less discrepant with the ejecta symmetry. Another possibility is that the ejecta asymmetry axis is the same as that of the line of sight. A clear, definitive determination of the nature of V842 Cen, in particular whether or not it is an IP and what its spin period is, will contribute to understanding the system and its ejecta morphology.

ACKNOWLEDGMENTS

We acknowledge the anonymous referee for the comments that helped improve the manuscript. We acknowledge Raimundo Lopes de Oliveira for useful tips and discussion about data analysis. This study is based on observations obtained with *XMM-Newton*, an ESA science mission with instruments and contributions directly funded by ESA member states and NASA.

REFERENCES

- Allan A., Hellier C., Beardmore A., 1998, *MNRAS*, 295, 167
 Brunschweiler J., Greiner J., Ajello M., Osborne J., 2009, *A&A*, 496, 121
 Buccheri R. et al., 1983, *A&A*, 128, 245
 Downes R. A., Duerbeck H. W., 2000, *AJ*, 120, 2007
 Fiedler R. L., Jones T. W., 1980, *ApJ*, 239, 253
 Gill C. D., O'Brien T. J., 1998, *MNRAS*, 300, 221
 Hoogerwerf R., Brickhouse N. S., Mauche C. W., 2005, in Buckley D. A. H., Warner B., eds, *ApJ*, 628, 946
 Livio M., 1995, in *ASP Conf. Ser. Vol. 85, Cape Workshop on Magnetic Cataclysmic Variables*. Astron. Soc. Pac., San Francisco, p. 80
 Moraes M., Diaz M. P., 2009, *AJ*, 138, 1541
 Morrison R., McCammon D., 1983, *ApJ*, 270, 119
 Mukai K., Kinkhabwala A., Paterson J. R., Kahn S. M., Paerels F., 2003, *ApJ*, 586, L77
 Pandel D., Córdova F. A., Mason K. O., Priedhorsky W. C., 2005, *ApJ*, 626, 396
 Scott A. D., 2000, *MNRAS*, 313, 775
 Sekiguchi K., Feast M. W., Fairall A. P., Winkler H., 1989, *MNRAS*, 241, 311
 Smith R. K., Brickhouse N. S., Raymond J. C., Liedahl D. A., 2001, *ApJ*, 556, L91
 Stute M., Luna G. J. M., Sokoloski J. L., 2011, *ApJ*, 731, 12
 Woudt P. A., Warner B., 2003, *MNRAS*, 340, 1011
 Woudt P. A., Warner B., Osborne J., Page K., 2009, *MNRAS*, 395, 2177
 Yuasa T., Nakazawa K., Makishima K., Saitou K., Ishida M., Ebisawa K., Mori H., Yamada S., 2010, *A&A*, 520, A25

³ See the latest catalogue of IPs at <http://asd.gsfc.nasa.gov/Koji.Mukai/iphome/catalog/alpha.html>.

This paper has been typeset from a $\text{\TeX}/\text{\LaTeX}$ file prepared by the author.